Article

Evaluation of the Cyclic Fatigue Resistance of Tia Tornado Blue and Tia Tornado Gold in Curved Canals: In Vitro Study

Ziyad Allahem *[ID]**, Mohammad Bendahmash, Reem Almeaither, Hussam Alfawaz and Abdullah Alqedairi** [ID]

Department of Restorative Dental Sciences, College of Dentistry, King Saud University,
Riyadh 11451, Saudi Arabia; mohammad.wd9@gmail.com (M.B.); reemalmeaither@gmail.com (R.A.);
halfawaz1@ksu.edu.sa (H.A.); aalqedairi@ksu.edu.sa (A.A.)
* Correspondence: zallahem@ksu.edu.sa

Abstract: (1) Background: The aim of this study was to investigate the cyclic fatigue behavior of the newly introduced endodontic instrument systems Tia Tornado Blue and Tia Tornado Gold. (2) Methods: The tested rotary instruments were divided according to their type into four groups as follows: Tia Tornado Blue (TTB), Tia Tornado Gold (TTG), Protaper Gold (PTG), and Vortex Blue (VB). The cyclic fatigue resistance of fifteen instruments of each group, totaling 60, was tested. Each instrument was rotated under continuous motion inside an artificial canal at simulated body temperature at the speed recommended by the manufacturer until fracture. The time to fracture was recorded, and the number of cycles to fracture (NCF) was calculated for each instrument. Additionally, the fractured segment length was calculated, and scanning electron microscopic (SEM) images were captured of the fractured surfaces. (3) Results: Statistical analysis revealed that the VB significantly had the highest NCF followed by the PTG, TTG, and TTB ($p < 0.05$). The lengths of the fractured segments were found to be similar among the tested instrument, which ranged from 4.42 to 4.86 mm ($p > 0.05$). SEM images exhibited the typical features of cyclic fatigue. (4) Conclusions: The newly introduced instruments, TTG and TTB, exhibited a significantly lower resistance to cyclic fatigue compared to the PTG and VB rotary instruments.

Keywords: cyclic fatigue; Tia Tornado Blue; Tia Tornado Gold; Protaper Gold; endodontic instrument

1. Introduction

Nickel titanium (NiTi) rotary instruments have been routinely used in endodontics practice since their innovation. Their priority in practice has been mostly due to the high flexibility, lower canal transportation, and reduced apical extrusion compared to stainless steel instruments [1,2]. However, NiTi fractures can happen during use due to many factors, although their prevalence is low and ranges from 0.7% to 3% [3,4].

Factors that have a crucial effect on the fatigue of NiTi instruments are the radius of curvature, the angle of curvature, operator skill, canal geometry, NiTi alloy, the heat treatment of the alloy, instrument size, the point of maximal instrument flexure, sterilization cycles, and manufacturing process [5–11]. Two mechanisms of fracture have been identified include cyclic fatigue and torsional fatigue. Cyclic fatigue is defined by the tension/compression cycles at the point of maximum flexure, while torsional fatigue is determined when an instrument tip or another part of the instrument is locked in a canal while the shank continues to rotate, and the torque goes beyond the elastic limit of the metal of the endodontic instrument [12,13].

According to reported findings, cyclic fatigue has been found to be the most frequent cause of failure [14–16]. Some new modifications have been made regarding endodontic instruments with advancements in the manufacturing processes of NiTi in attempts to reduce procedural errors and change the instrument performance in terms of the cyclic fatigue resistance. These modifications involved changes in heat treatments, alloy composition,

different cross-sectional design, thermomechanical processes, and surface treatment of the endodontic instruments [17–20].

In general, conventional NiTi instruments have an austenite structure at 37 °C degree body temperature. When the NiTi instrument is the control memory wire or M-wire, it is in the martensite phase [21]. The M-wire has been introduced to improve the flexibility to overcome complex curved canal anatomy. The M-Wire alloy is made of 508 nitinol wires that have been processed through a proprietary method of treatment consisting of drawing the raw wire under specific tension and heat treatments at various temperatures, thereby resulting in a material that includes some portions in both the martensitic and the premartensitic R phases while maintaining a pseudoelastic state [19,22].

The changes in heat treatment are made by changing the transition temperatures of the NiTi instruments, hence improving their cyclic fatigue resistance and flexibility, in comparison to the conventional superelastic NiTi instruments [13]. At human body temperature, traditional NiTi instruments have a lower finish temperature for austenite transformation (16–31 °C). However, thermally modified instruments have demonstrated increased austenite transformation finish temperatures (50–55 °C), which, in consequence, entails more martensitic components involved at body temperature [23].

Toward increasing the cyclic fatigue resistance, some manufacturers applied to NiTi heat-treated instruments a continuous heating and cooling process, thereby resulting in a surface oxidation layer that gives them a gold or blue appearance [24–26]. Gold and blue heated treatments enhance the fatigue resistance when compared with M-wire and conventional superelastic wires, and they are categorized as endodontic instruments with a superior martensite phase [27].

Vortex Blue (Dentsply Tulsa Dental, Tulsa, OK, USA) undergoes pre- and postmanufacture heat treatment, while Protaper Gold (Dentsply Maillefer, Baillagues, Switzerland) undergoes postmanufacture heat treatment [17].

The Tiadent manufacturer (Tiadent, Houston, TX, USA) provides several versions of rotary instruments with claimed superior strength and resistance to cyclic fatigue such as Tia Tornado Blue (TTB) (TTB; Tiadent, Houston, TX, USA) and Tia Tornado Gold (TTG) (TTB; Tiadent, Houston, TX, USA). The manufacturer also claims that the Tia Tornado Gold (TTG) wires are made from M-wire and are compatible with the ProTaper Gold (PTG) wires. It is imperative to understand the mechanical properties of the latest introduced instruments, as these can affect the clinician's choice in clinical management and predict their performance when preparing challenging root canal systems.

The newly introduced instruments provide a cost-efficient alternative to those commonly used in the dental office by dentist. To date, limited information is available on the mechanical properties of the TTB and TTG instruments. Therefore, the aim of this in vitro study was to investigate the cyclic fatigue behavior of the newly introduced rotary instruments TTB and TTG.

The null hypothesis was that there is no significant difference among the tested instruments in term of cyclic fatigue resistance.

2. Materials and Methods

2.1. Preparation of Artificial Canals

The artificial canals were made using the same technique used in the previous study by Alqedairi et al. [28]. The laser micromachining technique using the LASERTEC 40 (Deckel Maho Gildemeister, Hamburg, Germany), which consists of a Q-switched neodymium-doped yttrium aluminum garnet (Nd: Y3Al5O12 (Nd: YAG)) laser operating at a wavelength of 1064 nm with a maximum average power of 30 W, was used to make artificial canals in stainless steel plates with dimensions of 100 mm × 50 mm × 10 mm.

The artificial canal was modeled using CATIA V5® software (Dassault Systèmes, Version 5, Vélizy, France), and laser path programming was performed with a standard triangle language file of the proprietary machine software. After the process parameters

were established, the laser was focused on the block with the aid of a galvanometer scanner, and the canal was then machined layer by layer [29].

The artificial canals were prepared in stainless steel blocks with dimensions corresponding to the dimensions of the instrument tested: +0.1 mm in width and +0.2 mm in depth, with an angle of curvature of 60°, a radius of curvature of 5 mm, and a center of curvature 5 mm from the tip of the instrument.

2.2. Cyclic Fatigue Resistance Testing

The experiment was conducted according to a previous paper by Jamleh et al. [30]. Four different rotary instruments, PTG F2, VB 25.06, TTB 25.06, and TTG TF2, were tested in terms of cyclic fatigue resistance. Sample size calculation was performed based on previous studies [28,31] using G-power 3.1.9.4. Fifteen new instruments of each system were used in this study (Figure 1). All the selected instruments had a tip size of 0.25 mm and length of 25 mm. The experiment model was composed of an artificial canal that was milled in stainless steel block. The artificial canal had a maximum curvature point located 5 mm (D5) from the canal end. The metallic canal was covered with transparent glass to prevent the instrument from slipping out and to aid in visualizing the instrument when fracture occurred. The model was submersed in distilled water bath at temperature of 37 °C. X-Smart Plus (Dentsply Maillefer, Ballaigues, Switzerland) endodontic motor was used, and the instrument (19 mm in length) was inserted in the artificial canal. After the instrument was in place, the motor was operated at different speeds according to the manufacturers' instructions: TTB at 350 rpm, TTG at 300 rpm, PTG at 300 rpm, and VB at 500 rpm. The experiment was video recorded and time to fracture was calculated. The number of cycles to fracture (NCF) was calculated by multiplying the time to fracture in minutes by the tested system's rotational speed [30].
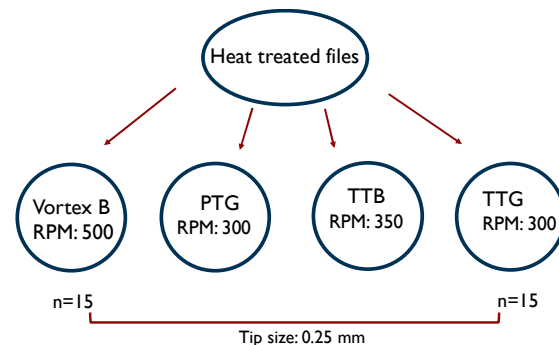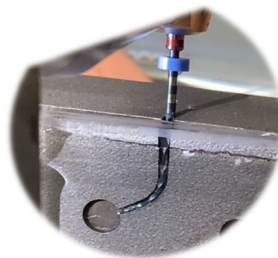

Figure 1. Flow chart of the experiment method for cyclic fatigue of an instrument in the artificial metal canal.

2.3. Scanning Electron Microscopy (SEM)

For the topographic features, one fractured instrument from each instrument system was selected, cleaned using alcohol, and dried at room temperature. Then, the instruments were mounted vertically on 15 mm metal stubs using double-sided carbon tape and subjected to microscopic analysis using SEM (SEM; 6360LV Scanning Electron Microscope;

JEOL, Tokyo, Japan) with 10 kV. The SEM photomicrographs were captured at different magnifications ranging from 150× to 1000×.

2.4. Statistical Analysis

Descriptive statistics were used to summarize the number of cycles to failure for each of the four groups. Normality of data was assessed using histograms, box–whisker plots, and a normality test (Shapiro–Wilk test). Distribution of data appeared to be normal, with normality test *p* values > 0.05.

Mean and standard deviation values are reported as descriptive statistics, and a one-way ANOVA test with Tukey's HSD was conducted to compare the groups.

3. Results

The mean NCF values, the outer diameter at the D5 and surface area of the tested instruments, are presented in Table 1. Using one-way ANOVA, a statistically significant difference between the groups was found ($p < 0.05$). A large effect size was found ($\eta^2 = 0.93$), thereby suggesting that the group accounted for 93% of the variability in the number of cycles to failure. Tukey's HSD showed that all the groups were significantly different from each other. The VB significantly had the highest NCF followed by the PTG, TTG, and TTB ($p < 0.05$) (Table 1). Moreover, the VB had the highest reliability (M = 1125.00), while the TTB had the lowest (M = 117.93).

Table 1. NCF: the diameter and the surface area of the instruments at the level of fracture of the experimental instrument systems. (n = 15).

Instrument System	Mean (±SD) (NCF)	Outer Diameter at D5 (mm)	Surface Area at D5 (mm^2)
VB	1125.00 ± 174.83 a *	1.9	0.22
TTB	117.93 ± 38.91 b	2	0.19
PTG	831.60 ± 79.88 c	2	0.23
TTG	542.80 ± 84.55 d	1.4	0.21

*: Different letters indicate a statistically significant difference ($p \leq 0.05$). NCF: number of cycles fracture.

There was no significant difference in the length of the fractured pieces among the groups; it ranged from 4.42 to 4.86 mm ($p > 0.05$). The outer diameter and the surface area of the instrument at the level of fracture were measured using a digital microscope (Hirox, Tokyo, Japan) (Table 1).

The SEM images exhibited the typical features of cyclic fatigue behavior (Figure 2). An area of fatigue striations (a) and another with a dimpled surface (b) were noticed. The crack usually initiated at the edge (A1, white arrow) and propagated to the fatigue striations (a). The instrument was weakened by the coalescence of the microvoids (B3, black arrows) produced, after which ductile fracture occurred, which was evident from the dimpled surface (b), until failure occurred. The round dimples indicated normal rupture patterns caused by tensile stresses.

The taper of each instrument was measured using a digital microscope (Digital Microscope, Hirox, Tokyo, Japan) (Figure 3). For the PTG, a steady increase in the degree of progressive taper was noticed from D0 to D5, whereas in the VB, a constant increase of 0.04 mm along the tested segment was recorded. On the other hand, the Tia Tornado Blue showed an irregular taper pattern, as there was no taper from D0 to D2. Then, an abrupt increase in the taper between D2 and D3, as well as D4 and D5, occurred. Lastly, the Tia Tornado Gold showed a similar result as the PTG. However, the increase in the taper was shown to be less steady as measurements were taken further from the tip. Looking at D4 and D5 specifically, the tapers between them in the VB and PTG were the same, which were 0.04. In the TTB and TTG, they were 0.07 and 0.09, respectively.
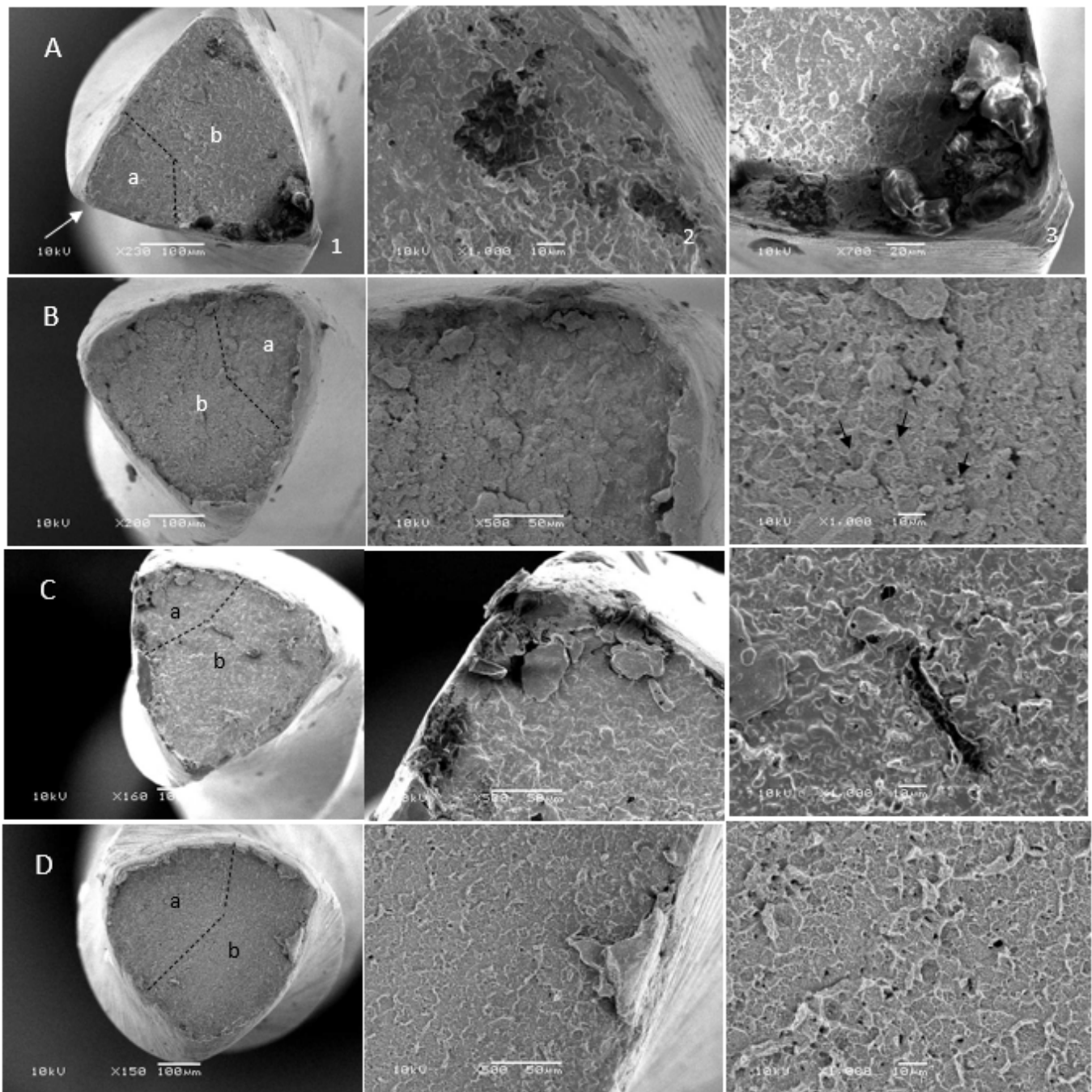
Figure 2. SEM of the cross-sections of the fractured surfaces. (**A**) TTB. (**B**) VB. (**C**) TTG. (**D**) PTG. SEM images exhibited typical features of cyclic fatigue, including (a) striations, (b) dimples, microvoids (black arrows), and initiation of cracks (white arrows).
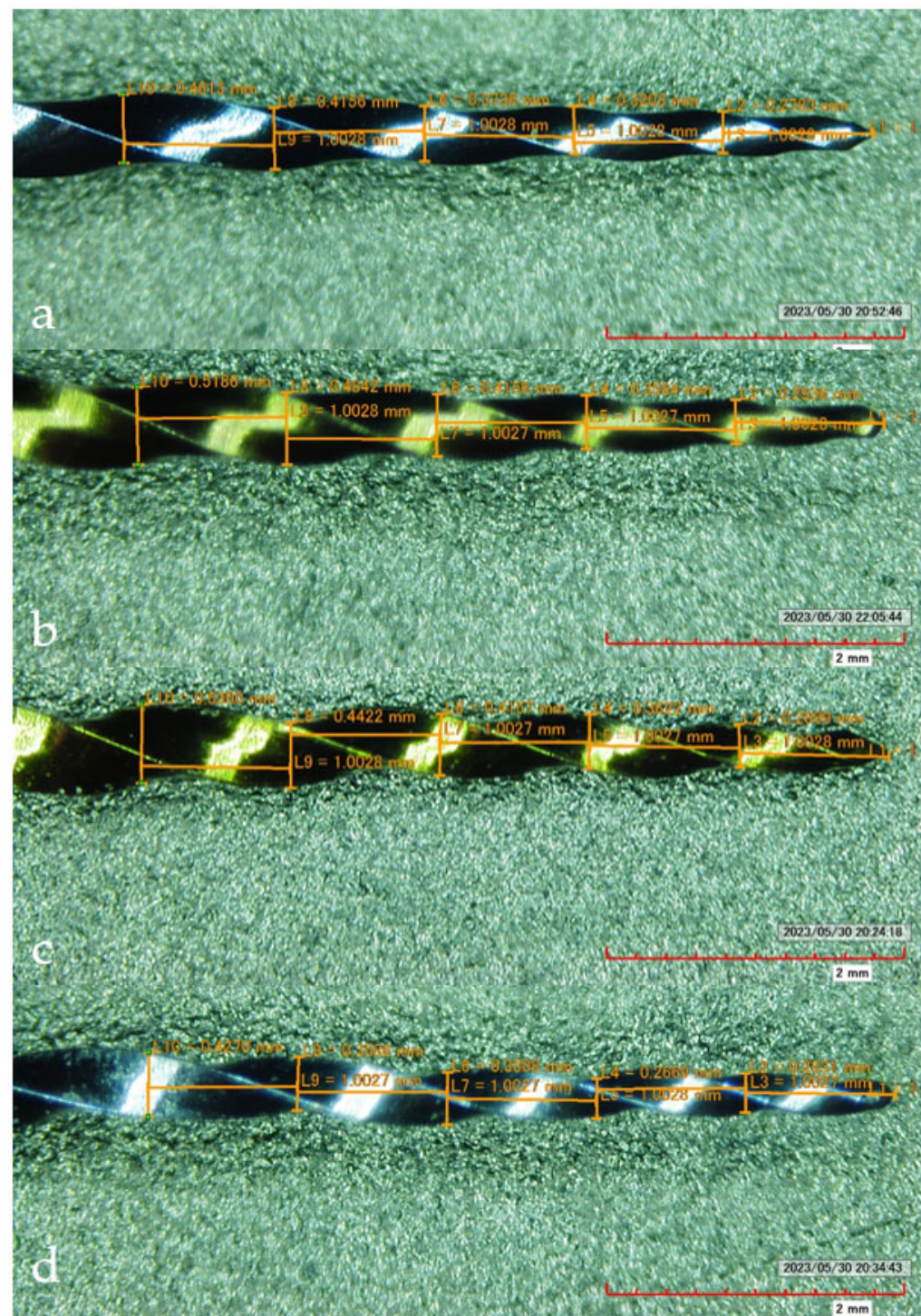
Figure 3. Measurements of each instrument taper from D0–D5 using a digital microscope. (**a**) VB. (**b**) PTG. (**c**) TTG. (**d**) TTB.

4. Discussion

Two new rotary systems, TTB and TTG, with a claim of possession of high fatigue resistance were tested in this study. The cyclic fatigue resistances of these instruments were compared to the VB and PTG, whose values are known in the market and feature enhanced resistance to cyclic fatigue [24–26]. The VB demonstrated a profound superiority of fatigue resistance compared to the other tested instruments. Furthermore, the PTG exhibited better fatigue resistance compared to the TTG and TTB.

A study by Uygun et al. 2020 found that there was no statistically significant difference between the VB and PTG, and this could be due to varied factors during the test like the difference in radius, which was 3 mm, while we used a 5 mm radius in this study [32]. Also, presenting a different result from our study, Sanchez et al. 2020, used a 5 mm radius and reported that the PTG had greater resistance than the CF compared to the VB. However, they used a synthetic oil designed for the lubrication of the artificial root canal systems instead of body temperature distilled water [33]. However, in agreement with our results, a study that used a synthetic oil and the same radius (5 mm) and angle of curvature (60 degrees) resulted in a superior NCF of the VB compared to the PTG [34].

SEM was used to visualize the broken fragments to verify that the topographic features were consistent with the cyclic fatigue failure. Typical cyclic fatigue features were seen with SEM, thereby identifying one or more crack initiation areas, fatigue striation, and a fast fracture zone with dimples [28].

To minimize the variables in this study, instruments with continuous rotation and a similar tip size were chosen. By considering the simulation of the clinical conditions and the complexity of the root canal system, a medium temperature of 37 °C and a 60-degree angle of curvature were used, as they may have crucial effects on cyclic fatigue resistance [5,31]. It was reported that increasing the temperature would have a significant influence on reducing the cyclic fatigue resistance [31]. Moreover, different medium solutions may impact cyclic fatigue resistance. Sodium hypochlorite (NaOCl), which is commonly used in root canal treatment, will lead to lower cyclic resistance, while an endodontic instrument performs with a similar cyclic resistance when placed in an ethylenediaminetetraacetic acid (EDTA) medium compared to distilled water [35]. In this study, body temperature distilled water was used as the medium.

The rotation speed of the instruments in this study was performed according to the manufacturers' instructions, as Pruett et al. reported that the rpm does not affect the cyclic fatigue resistance [5]. Static motion was used to compare the results with other studies, as the majority of studies used this method [3,4]. In static motion, flexural stress is generated mostly within a limited area, which is on the center of the curve and has less variables to change. On the other hand, in the dynamic motion, having the instrument move up and down while the instrument is rotating inside the artificial canal produces more cyclic resistance, as the stress occurs on a wider area of the instrument as the metal transforms while moving [3,4].

Cyclic fatigue is primarily caused by the propagation of faults from the metal surface until it leads to failure [7]. The low quality of the manufacturing can form microcracks and defects on the surface of the instrument [36]. When exposed to compression and tensile forces, the propagation of such defects can lead to metal fatigue, as these microcracks can act as stress concentration points [36]. These failures can be predicted by the stresses that are created by geometrical discontinuities, porosities, inclusions, and overheating during manufacturing [36]. According to Pruett et al., instruments separate at the point of maximum flexure, which is in accordance with our finding where most instruments fractured at 4–5 mm from the tip [5].

Different performance outcomes between the instruments with inferiority, as in the Tia Tornado, could be attributed to the chemical composition of the alloy, design features, and the quality of the manufacturing processes that the manufacturer did not disclose. The instrument cross-section, diameter, and surface area at the level of separation could play a significant role in fatigue behavior [36]. As shown in the results, the increases in taper for the Tia Tornado instruments at the point of failure were larger than those shown in the VB and PTG. It was reported that the taper/mm size affects the fatigue by concentrating the stresses over a short distance with a large taper, thereby making the instrument more prone to fracture [36]. The wider distance between the stress of tension and the stress of compression has been found to inversely affect fatigue failure, since it has a large total stress area [36]. Other factors that affect cyclic fatigue are flute design, circumference shape, flute depth, and the number of spirals [36].

Thermomechanical treatments enhance the instrument's performance in curved canals when exposed to cyclic compressions and tensions [19]. This improvement allows the instrument to show different crystal configurations based on the applied temperature and strain (martensite and austenite) [37]. It provides a martensitic phase at a lower temperature, which gives the instrument the flexibility and the cyclic fatigue resistance required [13,21].

From the results of the current study, the newly introduced instruments, TTG and TTB, need more improvements in terms of the cyclic fatigue before being used as alternatives for the VB and PTG in clinical settings. One of the limitations of this study was not including cutting efficiency and microhardness. However, future suggestions are to limit the variables more, which entails conducting the experiment at a similar speed between instrument groups and under a more simulated clinical condition like using a NaOCl medium instead of distilled water, in addition to clinical studies to determine the clinical outcome of endodontic treatment with the newly introduced instrument to be included in future studies.

5. Conclusions

The newly introduced rotary systems (TTB and TTG) failed to show any improvement in the cyclic fatigue resistance when compared to the VB and PTG. Therefore, the research hypothesis was rejected.

References

1. Puleio, F.; Bellezza, U.; Torre, A.; Giordano, F.; Lo Giudice, G. Apical Transportation of Apical Foramen by Different NiTi Alloy Systems: A Systematic Review. *Appl. Sci.* **2023**, *13*, 10555. [CrossRef]
2. Del Fabbro, M.; Afrashtehfar, K.I.; Corbella, S.; El-Kabbaney, A.; Perondi, I.; Taschieri, S. In Vivo and In Vitro Effectiveness of Rotary Nickel-Titanium vs. Manual Stainless Steel Instruments for Root Canal Therapy: Systematic Review and Meta-analysis. *J. Evid. Based Dent. Pract.* **2018**, *18*, 59–69. [CrossRef]
3. Alfouzan, K.; Jamleh, A. Fracture of nickel titanium rotary instrument during root canal treatment and re-treatment: A 5-year retrospective study. *Int. Endod. J.* **2018**, *51*, 157–163. [CrossRef]
4. Wang, N.N.; Ge, J.Y.; Xie, S.J.; Chen, G.; Zhu, M. Analysis of Mtwo rotary instrument separation during endodontic therapy: A retrospective clinical study. *Cell Biochem. Biophys.* **2014**, *70*, 1091–1095. [CrossRef] [PubMed]
5. Pruett, J.P.; Clement, D.J.; Carnes, D.L., Jr. Cyclic fatigue testing of nickel-titanium endodontic instruments. *J. Endod.* **1997**, *23*, 77–85. [CrossRef] [PubMed]
6. Parashos, P.; Linsuwanont, P.; Messer, H.H. A cleaning protocol for rotary nickel-titanium endodontic instruments. *Aust. Dent. J.* **2004**, *49*, 20–27. [CrossRef] [PubMed]
7. Kuhn, G.; Tavernier, B.; Jordan, L. Influence of structure on nickel-titanium endodontic instruments failure. *J. Endod.* **2001**, *27*, 516–520. [CrossRef] [PubMed]

8. Pereira, E.S.J.; Peixoto, I.F.C.; Viana, A.C.D.; Oliveira, I.I.; Gonzalez, B.M.; Buono, V.T.L.; Bahia, M.G.A. Physical and mechanical properties of a thermomechanically treated NiTi wire used in the manufacture of rotary endodontic instruments. *Int. Endod. J.* **2012**, *45*, 469–474. [CrossRef] [PubMed]

9. Alapati, S.B.; Brantley, W.A.; Svec, T.A.; Powers, J.M.; Nusstein, J.M.; Daehn, G.S. SEM observations of nickel-titanium rotary endodontic instruments that fractured during clinical Use. *J. Endod.* **2005**, *31*, 40–43. [CrossRef] [PubMed]

10. Topcuoglu, H.S.; Demirbuga, S.; Duzgun, S.; Topcuoglu, G. Cyclic fatigue resistance of new reciprocating files (Reciproc Blue, WaveOne Gold, and SmartTrack) in two different curved canals. *J. Investig. Clin. Dent.* **2018**, *9*, e12344. [CrossRef] [PubMed]

11. Zubizarreta-Macho, Á.; Alonso-Ezpeleta, Ó.; Albaladejo Martínez, A.; Faus Matoses, V.; Caviedes Brucheli, J.; Agustín-Panadero, R.; Mena Álvarez, J.; Vizmanos Martínez-Berganza, F. Novel Electronic Device to Quantify the Cyclic Fatigue Resistance of Endodontic Reciprocating Files after Using and Sterilization. *Appl. Sci.* **2020**, *10*, 4962. [CrossRef]

12. Hulsmann, M.; Donnermeyer, D.; Schafer, E. A critical appraisal of studies on cyclic fatigue resistance of engine-driven endodontic instruments. *Int. Endod. J.* **2019**, *52*, 1427–1445. [CrossRef] [PubMed]

13. Baird, E.; Huang, X.; Liu, H.; Hieawy, A.; Ruse, N.D.; Wang, Z.; Haapasalo, M.; Shen, Y. A novel model to evaluate the fatigue resistance of NiTi instruments: Rotational and axial movement at body temperature. *Aust. Endod. J.* **2023**, *49*, 301–307. [CrossRef] [PubMed]

14. Plotino, G.; Grande, N.M.; Cordaro, M.; Testarelli, L.; Gambarini, G. A review of cyclic fatigue testing of nickel-titanium rotary instruments. *J. Endod.* **2009**, *35*, 1469–1476. [CrossRef] [PubMed]

15. Cheung, G.S.P.; Peng, B.; Bian, Z.; Shen, Y.; Darvell, B.W. Defects in ProTaper S1 instruments after clinical use: Fractographic examination. *Int. Endod. J.* **2005**, *38*, 802–809. [CrossRef] [PubMed]

16. Shen, Y.; Zhou, H.; Campbell, L.; Wang, Z.; Wang, R.; Du, T.; Haapasalo, M. Fatigue and nanomechanical properties of K3XF nickel-titanium instruments. *Int. Endod. J.* **2014**, *47*, 1160–1167. [CrossRef] [PubMed]

17. Gavini, G.; Santos, M.D.; Caldeira, C.L.; Machado, M.E.D.L.; Freire, L.G.; Iglecias, E.F.; Peters, O.A.; Candeiro, G.T.D.M. Nickel-titanium instruments in endodontics: A concise review of the state of the art. *Braz. Oral Res.* **2018**, *32* (Suppl. S1), e67. [CrossRef] [PubMed]

18. Gambarini, G.; Pongione, G.; Rizzo, F.; Testarelli, L.; Cavalleri, G.; Gerosa, R. Bending properties of nickel-titanium instruments: A comparative study. *Minerva Stomatol.* **2008**, *57*, 393–398.

19. Larsen, C.M.; Watanabe, I.; Glickman, G.N.; He, J. Cyclic fatigue analysis of a new generation of nickel titanium rotary instruments. *J. Endod.* **2009**, *35*, 401–403. [CrossRef]

20. Ataya, M.; Ha, J.H.; Kwak, S.W.; Abu-Tahun, I.H.; El Abed, R.; Kim, H.C. Mechanical Properties of Orifice Preflaring Nickel-titanium Rotary Instrument Heat Treated Using T-Wire Technology. *J. Endod.* **2018**, *44*, 1867–1871. [CrossRef]

21. Shen, Y.; Zhou, H.M.; Zheng, Y.F.; Peng, B.; Haapasalo, M. Current challenges and concepts of the thermomechanical treatment of nickel-titanium instruments. *J. Endod.* **2013**, *39*, 163–172. [CrossRef] [PubMed]

22. Ye, J.; Gao, Y. Metallurgical characterization of M-Wire nickel-titanium shape memory alloy used for endodontic rotary instruments during low-cycle fatigue. *J. Endod.* **2012**, *38*, 105–107. [CrossRef] [PubMed]

23. Yahata, Y.; Yoneyama, T.; Hayashi, Y.; Ebihara, A.; Doi, H.; Hanawa, T.; Suda, H. Effect of heat treatment on transformation temperatures and bending properties of nickel-titanium endodontic instruments. *Int. Endod. J.* **2009**, *42*, 621–626. [CrossRef] [PubMed]

24. Elnaghy, A.M.; Elsaka, S.E. Mechanical properties of ProTaper Gold nickel-titanium rotary instruments. *Int. Endod. J.* **2016**, *49*, 1073–1078. [CrossRef] [PubMed]

25. Hieawy, A.; Haapasalo, M.; Zhou, H.; Wang, Z.J.; Shen, Y. Phase Transformation Behavior and Resistance to Bending and Cyclic Fatigue of ProTaper Gold and ProTaper Universal Instruments. *J. Endod.* **2015**, *41*, 1134–1138. [CrossRef] [PubMed]

26. Plotino, G.; Grande, N.M.; Cotti, E.; Testarelli, L.; Gambarini, G. Blue treatment enhances cyclic fatigue resistance of vortex nickel-titanium rotary files. *J. Endod.* **2014**, *40*, 1451–1453. [CrossRef] [PubMed]

27. Hou, X.M.; Yang, Y.J.; Qian, J. Phase transformation behaviors and mechanical properties of NiTi endodontic files after gold heat treatment and blue heat treatment. *J. Oral. Sci.* **2020**, *63*, 8–13. [CrossRef] [PubMed]

28. Alqedairi, A.; Alfawaz, H.; Bin Rabba, A.; Almutairi, A.; Alnafaiy, S.; Khan Mohammed, M. Failure Analysis and Reliability of Ni–Ti-Based Dental Rotary Files Subjected to Cyclic Fatigue. *Metals* **2018**, *8*, 36. [CrossRef]

29. Mohammed, M.K.; Al-Ahmari, A.; Umer, U. Multiobjective optimization of Nd:YAG direct laser writing of microchannels for microfluidic applications. *Int. J. Adv. Manuf. Technol.* **2015**, *81*, 1363–1377. [CrossRef]

30. Jamleh, A.; Alghaihab, A.; Alfadley, A.; Alfawaz, H.; Alqedairi, A.; Alfouzan, K. Cyclic Fatigue and Torsional Failure of EdgeTaper Platinum Endodontic Files at Simulated Body Temperature. *J. Endod.* **2019**, *45*, 611–614. [CrossRef]

31. Alfawaz, H.; Alqedairi, A.; Alsharekh, H.; Almuzaini, E.; Alzahrani, S.; Jamleh, A. Effects of Sodium Hypochlorite Concentration and Temperature on the Cyclic Fatigue Resistance of Heat-treated Nickel-titanium Rotary Instruments. *J. Endod.* **2018**, *44*, 1563–1566. [CrossRef]

32. Uygun, A.D.; Unal, M.; Falakaloglu, S.; Guven, Y. Comparison of the cyclic fatigue resistance of hyflex EDM, vortex blue, protaper gold, and onecurve nickel-Titanium instruments. *Niger. J. Clin. Pract.* **2020**, *23*, 41–45. [CrossRef]

33. Ruiz-Sánchez, C.; Faus-Llácer, V.; Faus-Matoses, I.; Zubizarreta-Macho, Á.; Sauro, S.; Faus-Matoses, V. The Influence of NiTi Alloy on the Cyclic Fatigue Resistance of Endodontic Files. *J. Clin. Med.* **2020**, *9*, 3755. [CrossRef]

34. Furlan, R.D.; Alcalde, M.P.; Duarte, M.A.; Bramante, C.M.; Piasecki, L.; Vivan, R.R. Cyclic and Torsional Fatigue Resistance of Seven Rotary Systems. *Iran Endod. J.* **2021**, *16*, 78–84.
35. Alfawaz, H.; Alqedairi, A.; Alhamdan, M.; Alkhzim, N.; Alfarraj, S.; Jamleh, A. Effect of NaOCl and EDTA irrigating solutions on the cyclic fatigue resistance of EdgeTaper Platinum instruments. *BMC Oral Health* **2022**, *22*, 195. [CrossRef]
36. McSpadden, J.T. *Mastering Endodontic Instrumentation*; Cloudland Institute: Chattanooga, TN, USA, 2007.
37. Pereira, É.S.J.; Viana, A.C.D.; Buono, V.T.L.; Peters, O.A.; de Azevedo Bahia, M.G. Behavior of nickel-titanium instruments manufactured with different thermal treatments. *J. Endod.* **2015**, *41*, 67–71. [CrossRef] [PubMed]